TISSUE ENGINEERING: Part A
Volume 17, Numbers 19 and 20, 2011

DOI: 10.1089/ten.tea.2010.0705

The Nell-1 Growth Factor Stimulates Bone Formation by Purified Human Perivascular Cells

Xinli Zhang, M.D., Ph.D.,[1,2] Bruno Péault, Ph.D.,[3] Weiwei Chen, Ph.D.,[1] Weiming Li, M.D.,[1] Mirko Corselli, Ph.D.,[3] Aaron W. James, M.D.,[1,2] Min Lee, Ph.D.,[4] Ronald K. Siu, M.S.,[5] Pang Shen,[3] Zhong Zheng, Ph.D.,[3] Jia Shen, Ph.D.,[1] Jinny Kwak, D.D.S.,[2] Janette N. Zara, M.D.,[3] Feng Chen, Ph.D.,[1] Hong Zhang, D.D.S.,[1] Zack Yin, D.D.S., Ph.D.,[1] Ben Wu, D.D.S., Ph.D.,[5] Kang Ting, D.M.D., DMedSci,[1–3,*] and Chia Soo, M.D.[3,*]

The search for novel sources of stem cells other than bone marrow mesenchymal stem cells (MSCs) for bone regeneration and repair has been a critical endeavor. We previously established an effective protocol to homogeneously purify human pericytes from multiple fetal and adult tissues, including adipose, bone marrow, skeletal muscle, and pancreas, and identified pericytes as a primitive origin of human MSCs. In the present study, we further characterized the osteogenic potential of purified human pericytes combined with a novel osteoinductive growth factor, Nell-1. Purified pericytes grown on either standard culture ware or human cancellous bone chip (hCBC) scaffolds exhibited robust osteogenic differentiation *in vitro*. Using a nude mouse muscle pouch model, pericytes formed significant new bone *in vivo* as compared to scaffold alone (hCBC). Moreover, Nell-1 significantly increased pericyte osteogenic differentiation, both *in vitro* and *in vivo*. Interestingly, Nell-1 significantly induced pericyte proliferation and was observed to have pro-angiogenic effects, both *in vitro* and *in vivo*. These studies suggest that pericytes are a potential new cell source for future efforts in skeletal regenerative medicine, and that Nell-1 is a candidate growth factor able to induce pericyte osteogenic differentiation.

Introduction

Stem cell research is a key driving force in the field of modern regenerative medicine. Identification and validation of new stem cell sources for tissue regeneration remains a critical part of these evolving endeavors.[1] Bone regeneration is critical to fracture repair as well as to healing of bone grafts used during spine, craniofacial, dental, post-trauma, and post-tumor reconstruction. However, current therapies either have high donor-site morbidity (e.g., bone autografts), limited efficacy (e.g., bone allografts), or are accompanied with undesirable or even severe adverse effects (e.g., treatments with bone morphogenetic proteins [BMPs]).[2–4] The highly orchestrated process of successful bone regeneration requires an optimal microenvironment specifically enriched with stem cells of osteogenic potential, osteoinductive growth factors, and suitable scaffolds to facilitate the regeneration of functional bone in the appropriate locations.[1,5]

Current conventional stem cell sources have significant drawbacks. Low stem cell numbers limit the use of fresh autologous bone marrow,[6,7] whereas the long culture derivation times hamper the use of bone marrow mesenchymal stem cells (BMSCs) or adipose-derived stem cells (ASCs). Although the use of the noncultured total stromal vascular fraction (SVF) from adipose tissues may remove the need for culture, available studies using SVF show lower bone regeneration efficacy relative to cultured ASCs.[8–10] Moreover, significant cell heterogeneity, including high numbers of nonstem cells, nonviable cells, and the presence of differentiation inhibiting endothelial cells[11,12] make the use of adipose total SVF less desirable. Thus, identification of readily available stem cell sources and development of well-defined stem cell differentiation protocols that comply with FDA regulatory requirements for product safety, purity, and potency comprise critical barriers to overcome before widespread application of cell-based regenerative medicine strategies.[1,13]

[1]Dental and Craniofacial Research Institute, University of California, Los Angeles, Los Angeles, California.
[2]Department of Orthodontics, University of California, Los Angeles, Los Angeles, California.
[3]UCLA and Orthopaedic Hospital Department of Orthopaedic Surgery and the Orthopaedic Hospital Research Center, University of California, Los Angeles, California.
[4]Division of Advanced Prosthodontics, Biomaterials, and Hospital Dentistry, University of California, Los Angeles, Los Angeles, California.
[5]Department of Bioengineering, University of California, Los Angeles, Los Angeles, California.
*These two authors are co-senior authors.

To directly address the issues related to stem cell availability, purity, and potency, we previously described the prospective purification of the perivascular ancestors of human MSC through fluorescence activated cell sorting (FACS) and delineated the native origins of at least some of these cells as being associated with capillaries and microvessels (i.e., pericytes).[14] This ability to prospectively isolate and characterize human multipotent stem cells, based on defined cell surface markers without need for culture, is significant due to the widespread tissue distribution of these cells, enabling large availability for autologous tissue engineering.[15] For instance, our unpublished data on uncultured perivascular stem cell yields from the SVF of human lipoaspirate samples agree with published ASC yields.[6,16,17] Moreover, we have confirmed that human perivascular cells sorted from diverse human tissues and cultured as single clones can give rise to adherent, multilineage progenitor cells that exhibit the features of MSC.[14] We show that these purified perivascular cells exhibit defined identity (CD146+, NG2+, PDGF-Rβ+, CD34−, CD45−, CD31−, CD56−) and purity. Importantly, purified perivascular cells also exhibit defined potency with respect to cell population doubling, *in vitro* chondrogenesis, *in vitro* adipogenesis, *in vitro* and *in vivo* myogenesis, and *in vivo* BMP-2 stimulated osteogenesis.[14] Interestingly, the purified perivascular cells also secrete more pro-angiogenic factors such as basic fibroblast growth factor and vascular endothelial growth factor (VEGF) than classically derived ASCs.[18]

It has been noted for decades, by ultrastructural analysis of regenerates, that these perivascular cells are actively involved in bone regeneration processes[19] and play critical roles in regulating endothelial cell function and angiogenesis.[20,21] However, it is unclear from our previous study if these implanted perivascular cells, as a novel source of stem cells, actually persist *in vivo* to differentiate and actively participate in angiogenesis and new bone formation. To better define the *in vivo* potency of this novel stem cell source, we describe here detailed tracking studies to determine the fate of the implanted human perivascular cells in the severe combined immunodeficient (SCID) mouse thigh muscle.

To ensure appropriate perivascular cell differentiation, we added Nell-1, a growth factor with novel osteoinductive properties. Animals deficient in functional Nell-1 demonstrate defects in skeletal[22] and vascular development (article in submission). For the past decade, the osteoinductivity of Nell-1 has been investigated and well-documented in several small and large animal models.[23–26] It is noteworthy that when injected into nude mouse muscle, Nell-1 promotes goat BMSC to regenerate bone that is structurally similar to native compact bone, whereas BMP2 induces a large hollow bone mass filled with fatty marrow tissue.[27]

In this present study, we use a model in which Nell-1 alone does not stimulate osteogenesis,[28] that is, mouse intramuscular transplantation, to definitively demonstrate that homogenously purified human pericytes possess significant osteogenic potential and that Nell-1 stimulation significantly enhances their proliferative, osteogenic, and angiogenic capacities during bone regeneration. Thus, the successful use of prospectively isolated human purified pericytes with Nell-1 is a proof of principle that critical clinical and regulatory barriers to musculoskeletal regenerative medicine can be addressed.

Materials and Methods

Purification of pericytes from human fetal pancreas

Pericytes were isolated from human fetal pancreas, known to house abundant pericytes.[14] Human fetal tissues were obtained following voluntary or therapeutic pregnancy interruptions performed at Magee-Womens Hospital (University of Pittsburgh), in compliance with Institutional Review Board protocol # 0506176. A single human fetus was used for the data presented herein. Using FACS, distinct microvessel pericytes (CD146+, CD34−, CD45−, CD56−) were isolated and then expanded *in vitro*. The antibodies for cell sorting include CD146 (AbD Serotec), CD34 and CD56 (BD Biosciences), and CD45 (Santa Cruz Biotechnology, Inc.). The purified pericytes were maintained in growth medium: F12–Dulbecco's modified Eagle's medium supplemented with 10% fetal bovine serum and 1× penicillin–streptomycin (Gibco). MSC markers were validated by flow cytometry throughout the cell expansion process. All experiments were done with passage 10 to 12 pericytes.

In vitro *proliferation and osteoblastic differentiation of human pericytes stimulated with rhNell-1*

Pericytes were cultured at low seeding density (2×10^3/well) in 96-well plates in the presence or absence of rhNell-1 (Aragen Bioscience) at 100 and 800 ng/mL for 7 days. Cellular proliferation was assayed every other day with MTT (Promega Corporation) in triplicate. For osteogenic differentiation, 1.5×10^5 pericytes per well were seeded in 24-well plates and cultured in growth medium supplemented with 50 μg/mL ascorbic acid and 10 mM beta-glycerol phosphatase. rhNell-1 at 100 and 800 ng/mL was added upon cell confluence and the fresh medium containing rhNell-1 was replenished every 3 days. Gene expression of osteoblastic cell markers, including *Runt-related transcription factor-2 (Runx2), Osterix (Osx)*, and *osteocalcin (OCN)* was detected at days 0, 3, 6, 9, and 12 poststimulation with rhNell-1 by real-time polymerase chain reaction (PCR) as stated in our previous work.[26] Gene expression of peroxisome *proliferator-activated receptor γ (PPARγ)* and *VEGF* was also detected by real-time PCR. The specific primers for real-time PCR were from TaqMan gene expression assays (Applied Biosystems). Mineralization was quantified by alizarin red staining as reported previously.[28]

Induction of pericyte mineralization on three-dimensional human cancellous bone chip scaffolds

A commercial human cancellous bone chip (hCBC) preparation (MTF) consisting of minimally processed hCBC mixed with demineralized bone matrix was used as a scaffold. About 2.5×10^5 pericytes were labeled with lentiviral green fluorescent protein (GFP) and seeded onto the surface of an hCBC scaffold that was supported by a Millicell culture insert (Millipore Corporation) in 24-well plates with minimum volume of growth medium. The same osteogenic differentiation media used for *in vitro* studies were supplied for this three-dimensional (3D) culture system after 2 h of cell seeding. The distribution and viability of seeded cells on hCBC were monitored by the morphology of GFP-positive cells. The fresh medium containing rhNell-1 at 100 ng/mL

was replenished every other day. The degree of mineralization was assessed using alizarin red staining described previously.[28] Images were obtained using an Olympus SZX12 fluorescence stereo microscope and an Olympus IX71 fluorescence inverted microscope.

Intramuscular implantation in SCID mice of pericytes loaded on hCBC with or without rhNell-1 preparation of implant

Each 15, 100, or 300 μg rhNell-1 protein total dose was lyophilized onto 50 mg tricalcium phosphate (TCP) particles 200–300 μm in diameter and stored at 4°C. The pericytes were labeled with RKH red fluorescent cell tracking dye (Sigma-Aldrich Co.) following manufacturer's instruction. Before implantation, the rhNell-1-loaded TCP was mixed well with hCBC carrier mechanically, and then 20 μL of 2.5×10^5 prelabeled pericyte suspension was dropped onto the mixed scaffold with gentle stirring to achieve a final volume of 100 μL for each implant. For live optical imaging experiments, pericytes were transduced with lentiviral luciferase instead of fluorescent labeling and mixed with hCBC before implantation into mouse thigh muscle. Treatment groups are further delineated in Table 1.

Surgical procedure

A muscle pouch implant in SCID mice was used to investigate ectopic bone formation. Twenty-four 6-week-old SCID mice were evenly and randomly divided into six experimental groups corresponding to the hCBC implant groups described (further delineated in Table 1). Thus, a total of four mice (or $n = 8$ muscle pouch implants) were performed per experimental group. Animals were anaesthetized by isoflurane inhalation (5% induction; 2% maintenance) and premedicated with 0.05 mg/kg buprenorphine.

Bilateral incisions in the hindlimbs were made, and pockets were cut in the biceps femoris muscles by blunt dissection, parallel to the muscle fiber long axis. For each mouse, 100 μL of material was implanted into each muscle pouch (2 sites) for a total of 200 μL per mouse. The fasciae overlying the muscle were sutured with a simple continuous pattern and the skin was closed in a separate layer using 4-0 or 5-0 Vicryl sutures in a subcuticular pattern. Animals were postoperatively treated with buprenorphine for 48 h and trimethorprim/sulfamethoxazole for 10 days for pain management and antibiotics, respectively. Animals were housed and experiments were performed in accordance with guidelines of the Chancellor's Animal Research Committee of the Office for Protection of Research Subjects at the University of California, Los Angeles.

Pericyte tracking after implantation

Pericytes expressing luciferase driven by a cytomegalovirus promoter were observed at 1, 2, and 3 weeks postoperation in mice from each experimental group. Bioluminescence imaging was performed using an IVIS Lumina II device (Caliper Life Sciences). Light outputs were quantified using Living Image software (version 2.5, Xenogen) as an overlay on Igor Pro imaging analysis software (WaveMetrics). Total light output, in photons/second/cm^2/steradian, was normalized to the integration time, the distance from the camera to the animal, the instrument gain, and the solid angle of measurement to provide for cross-platform comparison. Imaging was quantified by creation of circular regions of interest (ROIs) over each femur.

High-resolution quantitative microCT analysis

Samples were scanned using high-resolution micro-CT (Skyscan 1172F, Skyscan) at an image resolution of 19.73 μm (100 kV and 100 mA radiation source, using a 0.5 mm aluminum filter) and analyzed using DataViewer, Recon, CTAn, and CTVol software provided by the manufacturer. All quantitative and structural morphometric data use nomenclature described by the American Society for Bone and Mineral Research Nomenclature Committee.[29]

For 3D data analysis, ROI of diameter 7.18 mm were taken through the entire length of the scanned sample to quantify bone volume (BV). A value of 25 was selected as the optimal threshold that includes all mineralized tissue but excludes muscle and soft tissue in the scanned region. Sparsely mineralized bone tissue was further excluded by increasing the threshold value to 35 using a global thresholding procedure as described.[30,31] We designated the difference in BV obtained between thresholds 25 and 35 as the "volume of relatively new bone." Student's *t*-test was used to assess statistical difference in BV of the five experimental groups. 3D images were reconstructed for each threshold level and superimposed to separately represent all mineralized tissue from sparsely mineralized bone, and to highlight the volume of relatively new bone.

Histology and immunohistochemistry analysis

The decalcified tissues were embedded in paraffin. Deparaffinized sections were used for all histology and immunostaining. HE and trichrome staining were completed following standard protocols. Immunohistochemistry was performed with primary antibodies against bone sialoprotein (BSP) (Chemicon International), von Willebrand factor (vWF) (Abcam Inc.), VEGF, and MHC Class I antigen (Santa Cruz Biotechnology, Inc.) using the ABC (Vector Laboratories,

Table 1. Treatment Groups

Treatment	*Scaffold*	*rhNell-1*	*Pericytes*	n *(implants)*
Carrier Alone	hCBC (100 μL)	50 mg TCP alone	None	8
Nell-1 Alone	hCBC (100 μL)	15 μg Nell-1 in 50 mg TCP	None	8
Pericyte Alone	hCBC (100 μL)	50 mg TCP alone	2.5×10^5 in 20 μL	8
Pericyte + Nell-1	hCBC (100 μL)	15 μg Nell-1 in 50 mg TCP	2.5×10^5 in 20 μL	8
Pericyte + Nell-1	hCBC (100 μL)	100 μg Nell-1 in 50 mg TCP	2.5×10^5 in 20 μL	8
Pericyte + Nell-1	hCBC (100 μL)	300 μg Nell-1 in 50 mg TCP	2.5×10^5 in 20 μL	8

hCBC, human cortical/cancellous bone chip; TCP, tricalcium phosphate.

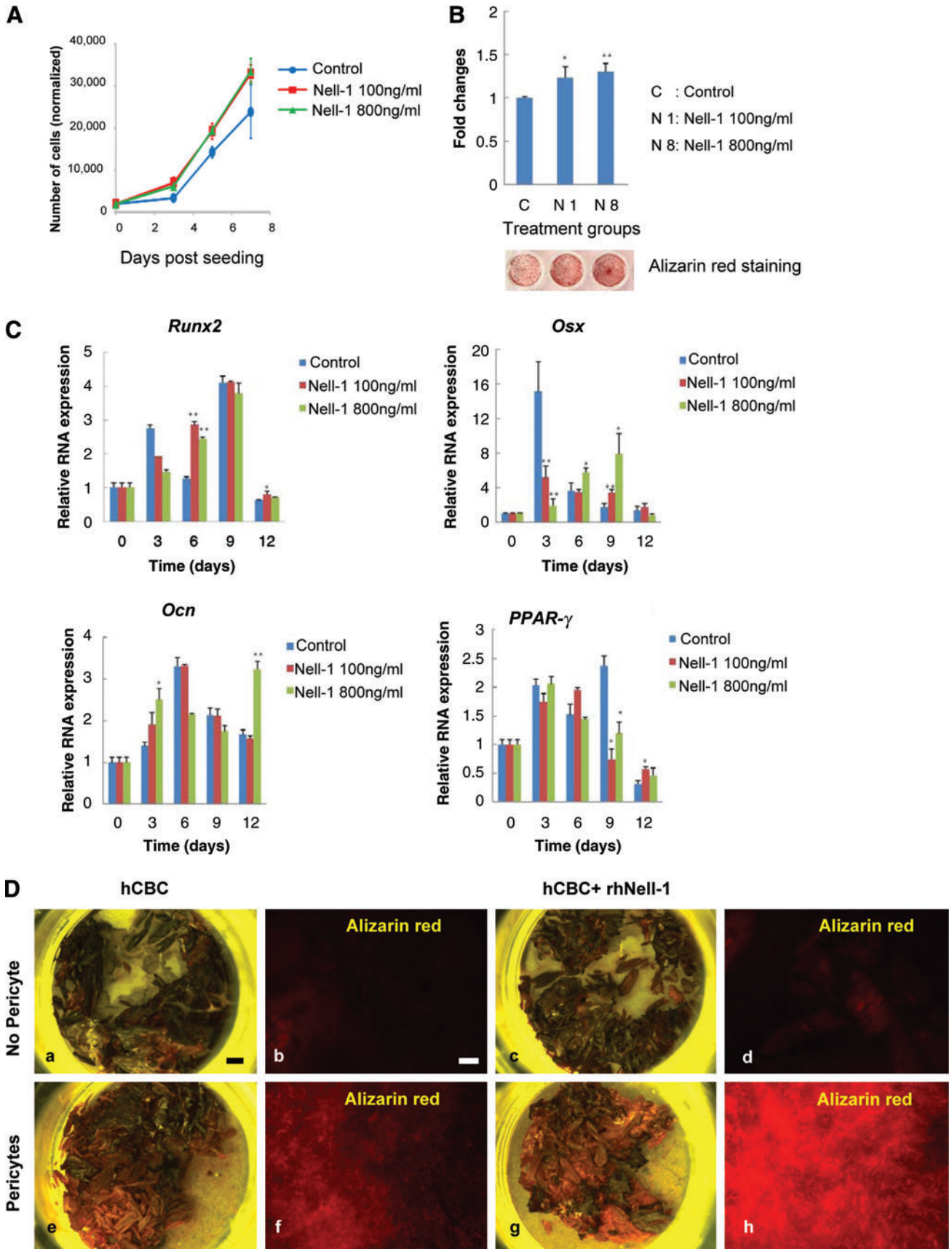
A
Number of cells (normalized)
40,000
30,000
20,000
10,000
0
0 2 4 6 8
Days post seeding
Control
Nell-1 100ng/ml
Nell-1 800ng/ml
B
Fold changes
2
1.5
1
0.5
0
C N 1 N 8
Treatment groups
C : Control
N 1: Nell-1 100ng/ml
N 8: Nell-1 800ng/ml
Alizarin red staining
C
Runx2
Relative RNA expression
Time (days)
Osx
Ocn
PPAR-γ
Control
Nell-1 100ng/ml
Nell-1 800ng/ml
D
hCBC
hCBC+ rhNell-1
No Pericyte
Pericytes
Alizarin red
a
b
c
d
e
f
g
h

Inc.) method. Frozen sections used for *in situ* human pericyte tracking were counterstained with Hoechst 33324 (Sigma-Aldrich Co.). The histological images were obtained on an Olympus BX51 fluorescence microscope. Semi-quantitative histomorphometric analysis of H&E, vWF, and VEGF stains was performed as previously described.[32]

Statistical analysis

Statistical analysis was performed using an appropriate analysis of variance (ANOVA), followed by *post hoc* analysis between specific groups. A Bonferroni adjustment was performed to ensure significance when multiple groups were examined. For data presented in 1B, a one-factor ANOVA was used (treatment type), whereas in all other figures a two-factor ANOVA was used (treatment type and time in days).

Results

Nell-1 enhances human fetal pericyte proliferation and osteoblastic differentiation in vitro

In the current study, human fetal pancreatic perivascular cells at passages 10 to 12 were used for all experiments. To determine the effect of Nell-1 on proliferation, perivascular cells were stimulated with rhNell-1 at 100 and 800 ng/mL under regular growth culture conditions. Both dosages induced significantly greater proliferative activity as early as 3 days poststimulation (Fig. 1A). Functionally, rhNell-1 also significantly increased the mineralization of pericytes as revealed by alizarin red staining (Fig. 1B). To gain insight into pericyte osteoblastic differentiation induced by rhNell-1, the expression of the major osteoblastic cell markers *Runx2, Osx*, and *OCN* as well as the adipogenic differentiation gene *PPARγ* were evaluated using real-time PCR (Fig. 1C). In response to Nell-1 stimulation, *Runx2* and *Osx* expression levels transiently decreased in the early phase (day 3), elevated at the mid phase (day 6 and/or day 9), and then returned to low levels as mineralization occurred. Nell-1 stimulation also upregulated *Ocn* expression at both early and late stages. In contrast, the adipogenic master transcriptional factor *PPARγ* expression was significantly reduced at day 9. To investigate the compatibility of pericytes and hCBC scaffold carrier, the osteoblastic differentiation of pericytes cultured on hCBC was quantified by alizarin red staining at day 15 after rhNell-1 stimulation. The degree of mineralization was greatest in pericytes + hCBC + rhNell-1 groups, followed by pericytes + hCBC (Fig. 1D). These data demonstrate that pericytes undergo osteogenic differentiation in 3D scaffolds, and that rhNell-1 stimulation significantly enhances osteogenic, while inhibiting adipogenic gene expression.

Nell-1 promotes pericyte osteochondrogenic differentiation and endochondral bone formation in vivo

We next examined the effects of rhNell-1 on bone formation by perivascular cells *in vivo*. Because Nell-1 can promote bone formation in many osseous defect models, we specifically utilized a muscle pouch implantation model in which Nell-1 alone was unable to promote bone formation without adding exogenous osteoprogenitor cells.[27,28] This allowed a more direct assessment of human pericyte osteogenic potential when in the presence and absence of rhNell-1. Fixed-volume 100 μL implants in different treatment groups were implanted into thigh muscles of immunodeficient mice. Histology revealed clear differences in endochondral bone formation as early as 2 weeks postimplantation. hCBC alone and hCBC + 15 μg rhNell-1 samples manifested very limited chondrogenesis (Fig. 2A–F), whereas the hCBC + pericytes group exhibited robust chondrogenesis (Fig. 2G–I). Meanwhile, hypertrophic cartilage with mineralized matrix surrounding marrow-like cells was readily detectable in hCBC + pericytes + 15 μg rhNell-1 samples (Fig. 2J–L). To further explore rhNell-1's role in promoting bone regeneration by hCBC + pericytes, higher rhNell-1 doses of 100 and 300 μg were also tested in addition to rhNell-1 at 15 μg. At 4 weeks postimplantation, there was abundant new bone formation surrounding almost every hCBC particle with intense positive BSP staining in the higher dose rhNell-1 groups, whereas rhNell-1 at 15 μg promoted a lesser amount of bone generation (Fig. 2M–R).

Quantitative microCT analysis at 4 weeks revealed distinct differences in new bone formation. Isolated hCBC particles demonstrated minimal connectivity, whereas hCBC + rhNell-1 and hCBC + pericytes regenerates exhibited increased particle consolidation that was accompanied by increased new bone in hCBC + rhNell-1, and, interestingly, decreased new bone formation in the hCBC + pericytes group (Fig. 3A–C, F). In contrast, both the 15 and 300 μg hCBC + pericytes + rhNell-1 samples demonstrated significantly increased hCBC particle consolidation as well as new bone formation (Fig. 3D–F). These data indicate that Nell-1 coupled with responsive stem cells, such as pericytes, markedly accelerated chondrogenic and osteogenic differentiation and increased new bone formation. In addition, histomorphometric analysis of serial histological sections demonstrated a significant increase in bone formation, especially among pericyte + rhNell-1 groups (Fig. 3G). The significant decrease in new bone formation in the hCBC + pericytes group relative to hCBC alone was unexpected, and suggests that rhNell-1, beyond supporting perivascular stem cell differentiation (Fig. 2J–R) and proliferation (Fig. 1A), may also support perivascular stem cell survival. Decreased new bone formation in the hCBC + rhNell-1 vs. hCBC + pericytes + rhNell-1 samples is consistent with our earlier *in vitro* observations of lesser cell numbers and/or decreased osteogenic response of retained hCBC cells relative to purified perivascular cells (Fig. 1D).

Nell-1 promotes engraftment and tissue integration of purified pericytes in vivo

To directly assess the impact of Nell-1 on purified perivascular cells *in vivo*, the pericytes were transduced with

FIG. 1. Enhanced *in vitro* proliferation and osteoblastic differentiation of purified human perictyes with Nell-1 stimulation. **(A)** Significantly increased pericyte proliferation was seen with Nell-1 stimulation. **(B)** Pericytes underwent mineralization in osteoblastic differentiation medium and this potential was significantly enhanced by Nell-1. **(C)** Real-time polymerase chain reaction of osteoblastic marker genes *Runx2, Osx,* and *Ocn* as well as adipogenic marker gene *PPARγ* during pericyte osteoblastic differentiation. **(D)** Pericyte mineralization on three-dimensional hCBC scaffold evaluated by Alizarin red staining. Scale bars: 1 mm for **(a, c, e, g)** images from a stereo microscope and 100 μm for **(b, d, f, h)** images from an inverted microscope. hCBC, human cancellous bone chip. Color images available online at www.liebertonline.com/tea

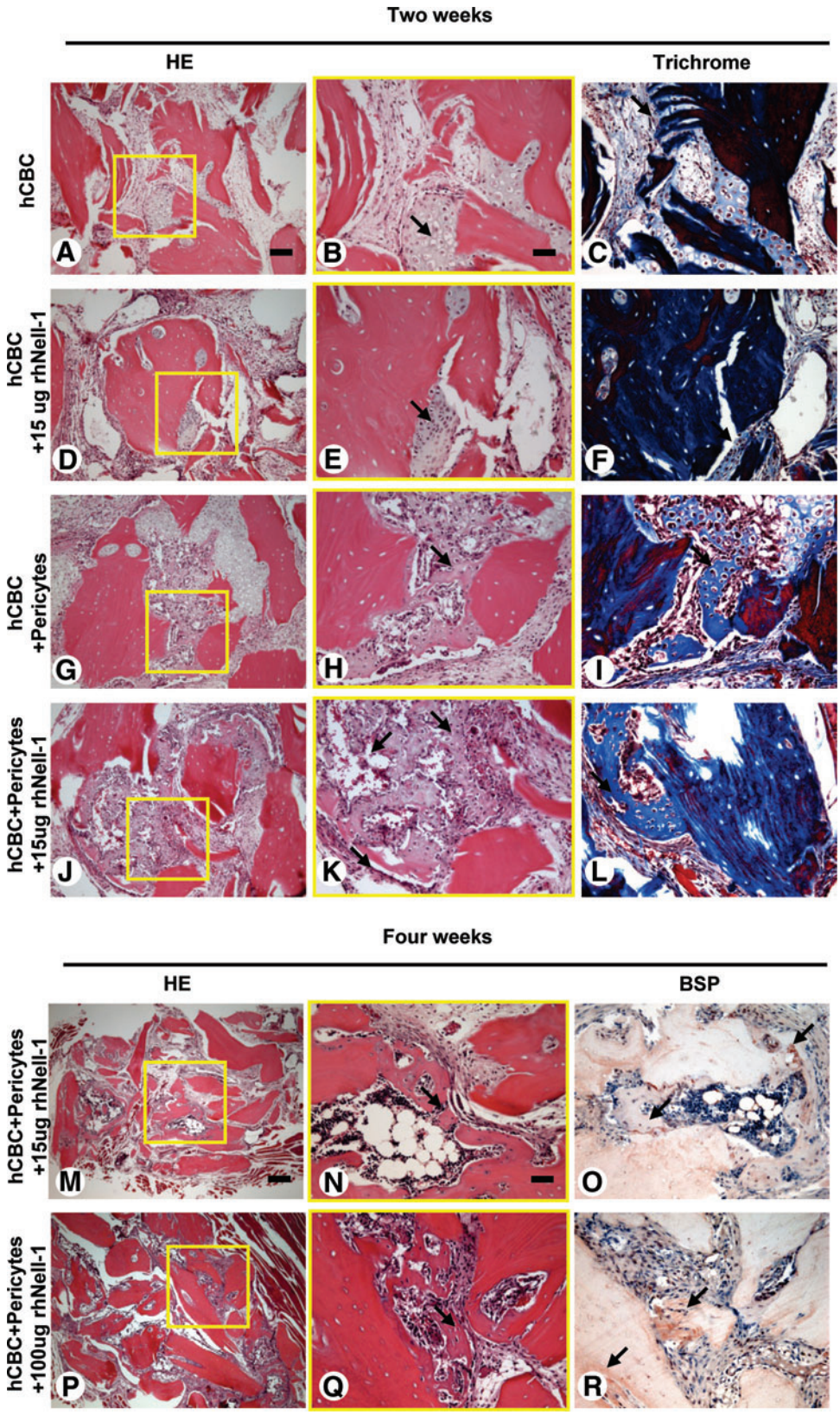

FIG. 2. Histology of bone regenerates with involvement of purified pericytes and Nell-1. **(A–F)** Only small amounts of cartilaginous tissue (arrows) formed in hCBC alone and hCBC + rhNell-1 implants without loaded pericytes at 2 weeks postoperation. **(G–L)** Large amount of cartilaginous tissue and focal mineralized woven bone (arrows) formed in pericyte-loaded hCBC implants with even more mineralized bone with Nell-1 presence. **(M–R)** At 4 weeks postoperation, new bone formation with bone sialoprotein positive staining (arrows) occurred at almost every pericyte-loaded hCBC scaffold implant with the higher rhNell-1dose. Scale bars: 100 μm for **A, D, G,** and **J**; 50 μm for **B, C, E, F, H, I, K, L, N, O, Q,** and **R**; and 250 μm for **M** and **P**. Color images available online at www.liebertonline.com/tea

lentiviral luciferase before implantation with hCBC or hCBC + rhNell-1 into mouse thigh muscles for detailed tracking studies. Luciferase activity was monitored by weekly optical imaging for 3 weeks. Bioluminescence imaging demonstrated optical signals largely confined to the implant vicinity. Excitingly, signal intensity from the transduced pericytes increased in an rhNell-1 dose-dependent fashion. Relative to no rhNell-1, signal intensity was 15.2-fold higher in the 300 μg and 6.3-fold higher in the 15 μg groups at 6 days. High signal levels persisted in the 300 μg group for at least 21

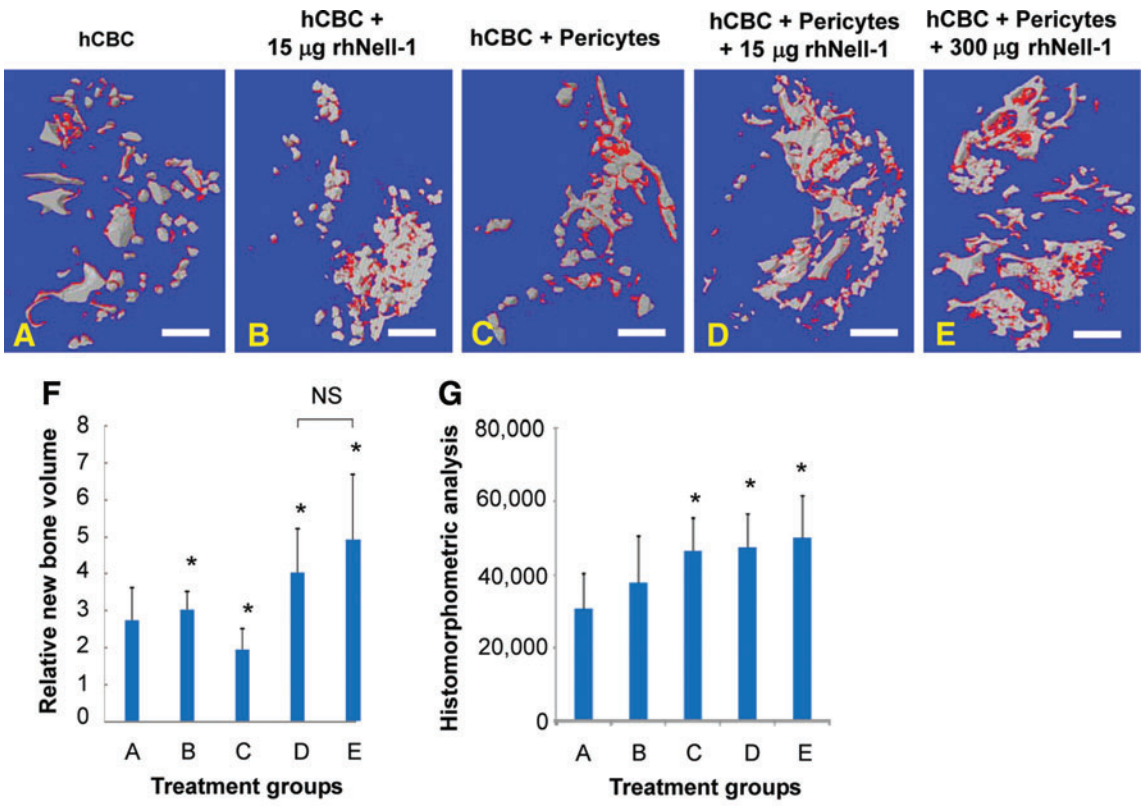

FIG. 3. MicroCT analysis of new bone regeneration. **(A)** Scattered and isolated hCBC scaffold particles (in gray) were observed in hCBC alone implants with some new bone (in red). **(B, C)** Increased hCBC particle convergence and small cluster formation when rhNell-1 was applied with hCBC **(B)** or when pericytes were loaded onto hCBC **(C)**. **(D, E)** Significant hCBC particle convergence forming large clusters with obvious new bone formation (in red) when pericyte-loaded hCBC was applied together with rhNell-1. **(F)** Quantitation of new bone formation among different treatment groups, $*p < 0.05$ versus group A of hCBC alone and NS: no significant difference. Scale bars: 2 mm. **(G)** Histomorphometric analysis of bone formation, represented as pixels bone by H&E staining per high-power field, $n = 10$ per group. Color images available online at www.liebertonline.com/tea

days (Fig. 4A, B). These data indicate that Nell-1 promotes either pericyte survival, engraftment, and/or proliferation, and are consistent with *in vitro* data showing Nell-1 enhancement of pericyte proliferation (Fig. 1A)

Tissue integration of the human pericytes was also investigated by prestaining the cells with RKH, a red fluorescent live cell labeling dye, before implantation. At 4 weeks postimplantation, the prestained pericytes were still clearly visible in areas of active regeneration and mineral deposition on the surface of hCBC particles (Fig. 5A–F) (yellow arrows) as well as in perivascular areas next to endothelial cells (Fig. 5G–I) (red arrows). To further confirm the relative contribution of engrafted RKH+pericytes to blood vessel formation, we stained for CD31 on endothelium and superimposed with RKH labeling images (Fig. 5J–L). Staining with the endothelial cell marker CD31 confirmed that pericytes are also found in close association to blood vessels, therefore recapitulating their original localization. These data conclusively demonstrate human pericyte engraftment, persistence, and integration in and around new bone tissue.

Nell-1 stimulates angiogenic effects in pericytes at early stages of bone regeneration

Pericytes interact with endothelial cells to stabilize newly formed endothelial tubes and regulate endothelial cell proliferation, differentiation, migration, and survival. Hence, the participation of pericytes in angiogenesis is not unexpected. One intriguing question, however, is whether Nell-1 can enhance the angiogenic function of purified perivascular cells. Besides defects in skeletal development,[22] functionally Nell-1-deficient mouse embryos also exhibit defective vasculogenesis during mid-gestation (personal communication from Dr. Cymbeline Culiat). Interestingly, when human pericytes were maintained in osteogenic differentiation medium, rhNell-1 was capable of further upregulating *VEGF* expression starting at day 6 and throughout the study period (Fig. 6A). *In vivo* angiogenic function of the pericyte+rhNell-1 combination was assessed by histology and vWF endothelial staining of hCBC+pericytes±rhNell-1 specimens at 1 week postimplantation, a time shown to be optimal for monitoring *in vivo* angiogenesis.[33] The hCBC+pericytes+rhNell-1 group exhibited relatively higher capillary and small blood vessel numbers and density in the granulation tissues surrounding the hCBC particles as well as significantly more positive vWF endothelial staining relative to the hCBC + pericytes group. Specifically, vWF staining intensity was assessed by histomorphometric analysis of serial sections ($n = 4$ per group), showing a clear and abundant increase in relative staining intensity with pericyte addition to hCBC. (Fig. 6B–F). Meanwhile, VEGF immunohistochemistry was performed on samples at 2 weeks postimplantation. VEGF staining was

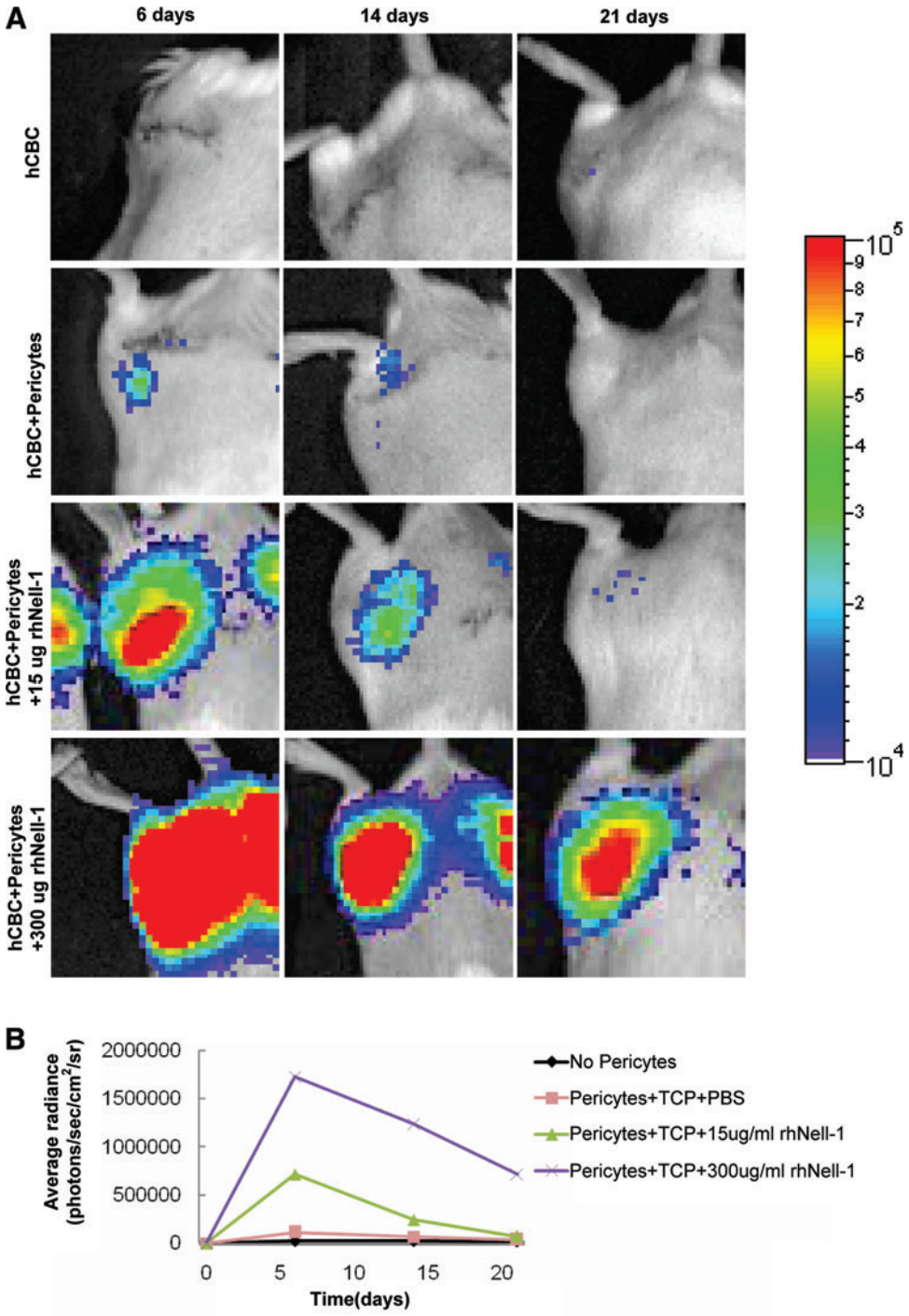

FIG. 4. *In vivo* tracking of human pericytes implanted intramuscularly in SCID mice. **(A)** Panel of optical images was obtained at different time points for tracking human pericytes transduced with lentiviral luciferase after implantation in thigh muscles of SCID mice. Notably, the signals were remarkably higher in rhNell-1 groups in a dose-dependent manner. **(B)** Quantitation of the optical signals from implanted human pericytes among different treatment groups. SCID, severe combined immunodeficient; TCP, tricalcium phosphate. Color images available online at www.liebertonline.com/tea

localized mainly to the periphery along hCBC particles and the stromal tissues surrounding active bone formation sites (Fig. 6G–I). Notably, the hCBC controls exhibited only low levels of VEGF staining, whereas the pericyte groups demonstrated abundant VEGF signals with highest signals in the hCBC + pericytes + rhNell-1 group (Fig. 6I). The semi-quantitation analysis showed a 139% increase in staining intensity among pericyte engrafted groups (means 9907 pixels, 23,762 pixels, and SDs 3657, 8457, respectively), and a 186% increase among pericyte + rhNell-1 groups (means 9907 pixels, 28,317 pixels, and SDs 3657, 13,048, respectively; $n = 4$ per group). To determine if the VEGF signals originated from the implanted human cells or host murine cells and to document the spatial relationship between VEGF signals and implanted pericytes, serial tissue sections used for VEGF immunostaining were further labeled with an anti-human MHC Class I antibody. MHC Class I–positive pericytes, indicating human origin, were localized in areas of high VEGF staining (Fig. 6J–L). However, the significantly more prevalent distribution of VEGF signals, relative to that of human pericytes, indicates that the host stromal cells are also involved in production of VEGF. These data demonstrate that implanted human

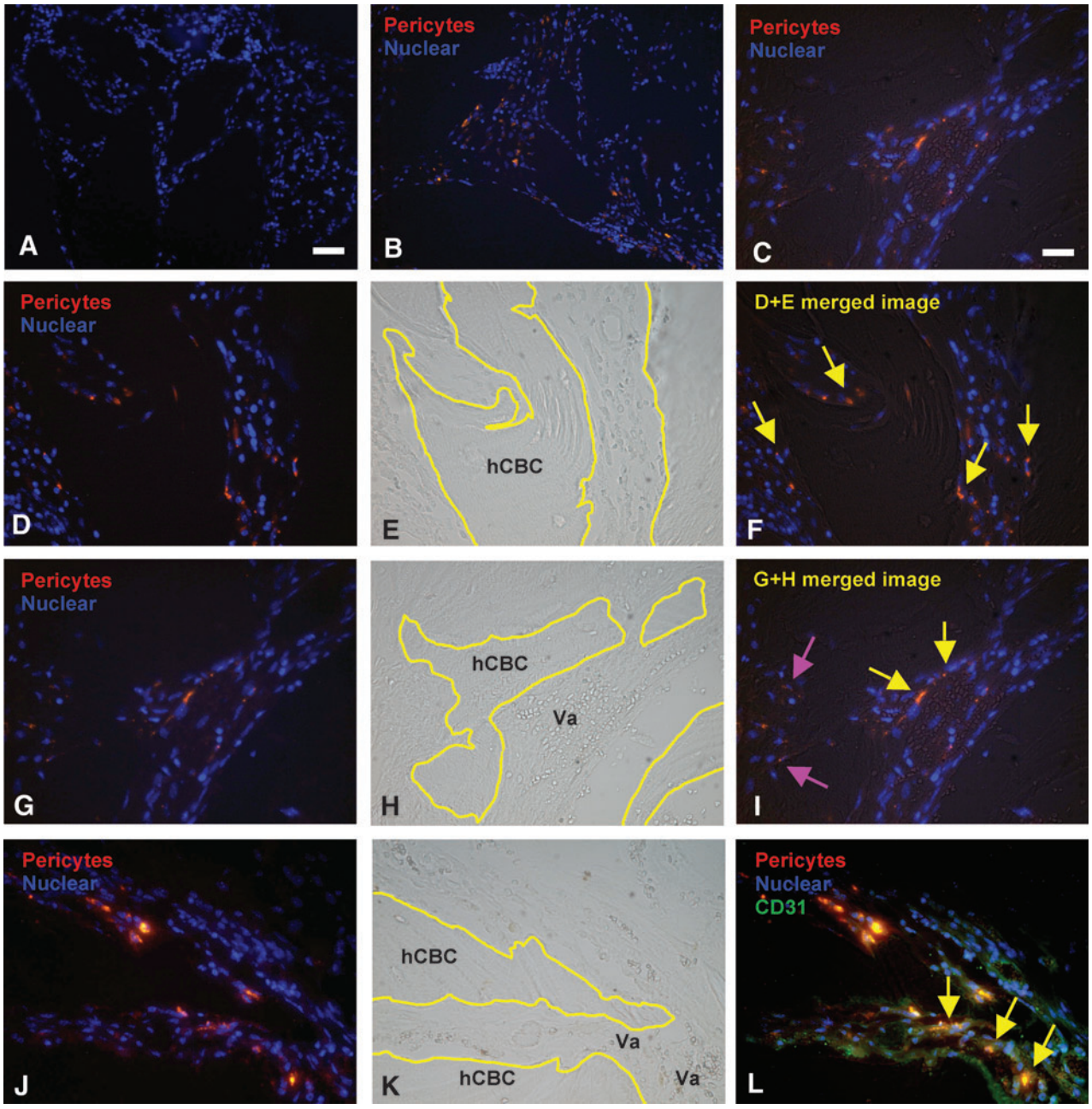

FIG. 5. Tissue engraftment of implanted human pericytes into regenerates. **(A)** Images of implants without loaded human pericytes onto hCBC showed cell nucleus stained with Hoechst 33342 (in blue). **(B)** The RKH live cell dye prelabeled human pericytes (in red) were clearly visible in the implants of pericyte-loaded hCBC groups at 4 weeks postintramuscular implantation. **(C)** Higher magnification of image **B**. **(D)** Prelabeled human pericytes (in red) in hCBC + rhNell-1 implants. **(E)** Phase-contrast image **D** showing hCBC particles outlined in yellow lines and tissue profile. **(F)** Superimposed image of **D** and **E** showing implanted pericytes engrafted into remodeling hCBC scaffolds (yellow arrows). **(G–I)** Prelabeled human pericytes not only engrafted into remodeling hCBC scaffolds (pink arrows), but also participated in vascularization (yellow arrows). **(J–L)** Prelabeled pericytes combined with CD31 immunohistochemistry (in green), showing colocalization (yellow arrows). Scale bar: 50 μm for **A** and **B**, and 25 μm for **C–I**.

pericytes possess angiogenic and trophic properties that are significantly enhanced by rhNell-1 during bone regeneration.

Discussion

Pericytes—or mural cells—are closely associated anatomically with endothelial cells in the walls of capillaries and microvessels in all vascularized tissues throughout the human body. Arguably, pericytes may represent a primitive origin of hMSC since they share phenotypic traits with MSC,[34–38] express all the markers of hMSC *in situ*, and are indistinguishable from conventionally derived hMSC after purification to homogeneity and cultivation *in vitro*.[14,39] Pericytes purified from different human tissues possess similar, if not identical, multipotency for inducible differentiation into

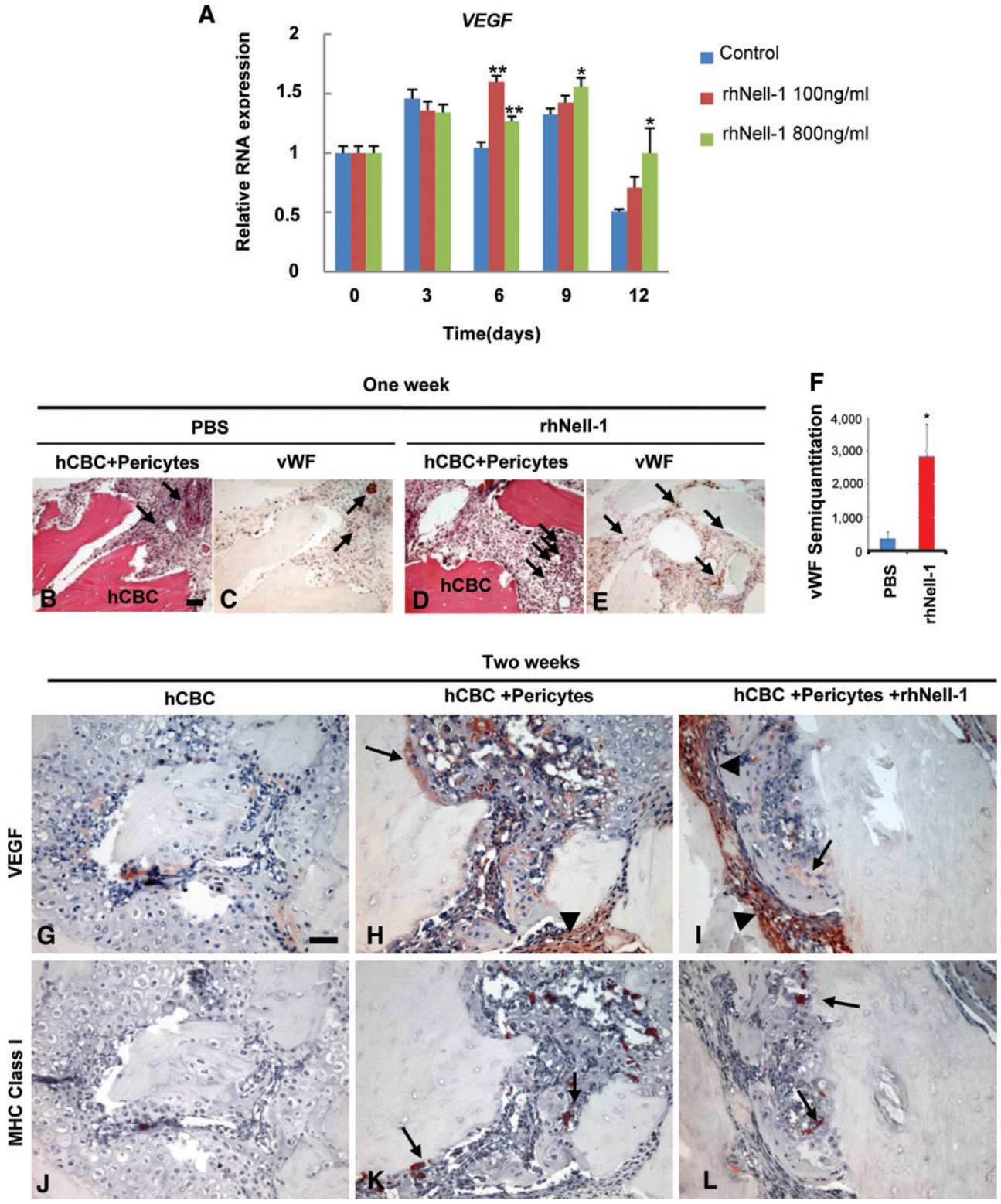

FIG. 6. Angiogenic effects of purified human pericytes during osteoblastic differentiation *in vitro* and *in vivo*. **(A)** *VEGF* mRNA expression of purified pericytes was significantly enhanced with rhNell-1 stimulation during osteoblastic differentiation. **(B, C)** HE and vWF immunohistochemistry in hCBC + pericytes + PBS samples. **(D, E)** HE and vWF immunohistochemistry in hCBC + pericytes + rhNell-1 samples. **(F)** Semi-quantification of vWF immunostaining. **(G–I)** Immunohistochemistry of VEGF (arrows) in 2 week samples from indicated treatment groups. **(J–L)** Immunohistochemistry of human MHC Class I showing implanted human pericytes in 2-week samples from indicated treatment groups. Scale bar: 50 μm for **B–E** and **G–L**. $^{*}p < 0.05$, $^{**}p < 0.01$. Black arrows and arrowheads indicate regions of positive staining. VEGF, vascular endothelial growth factor; vWF, von Willebrand factor. Color images available online at www.liebertonline.com/tea

myogenic, adipogenic, chondrogenic, and osteogenic cell lineages.[14,18] Notably, BMSC and muscle derived stem cells may also contain a fraction of perivascular cells as they have all exhibited robust osteogenic potential in previous reports.[40–42] In our present study, we utilized the pericytes derived from tissues (i.e., pancreas) not typically associated with bone formation to illustrate their osteogenic potential.

The data shown here not only validate the *in vitro* osteogenicity of human pericytes derived from pancreas, but also definitively demonstrate their *in vivo* angiogenic and trophic effects. Specifically, the osteogenic capacity of purified human pericytes was strongly evidenced by *Runx2, Osx,* and *Ocn* gene expression and mineralization *in vitro*, whereas VEGF production in osteoblastic differentiation medium confirmed their concomitant angiogenic properties. *In vivo*, the pericytes also demonstrated their capacity for tissue engraftment and trophic effects through, in part, VEGF production and by induction of VEGF production by host cells.

Remarkably, Nell-1 stimulation significantly promoted pericyte survival/engraftment as well as angiogenic and osteogenic properties. Interestingly, Nell-1 was mitogenic for human pericytes, in contrast to other cell types,[27,43,44] indicating that Nell-1-induced proliferation is cell and/or differentiation state dependent. Nell-1 mitogenic effects on human pericytes may also account for much higher luciferase signals and increased bone regeneration volumes in the mouse muscle pouch. In general, stem cells do not form bone unless they are precultured under osteogenic conditions or treated with osteoinductive factors.[45] Since Nell-1 reproducibly induced bone regeneration in various small and large animal studies,[23–26] the use of rhNell-1 ensures an appropriate proliferative and osteoinductive microenvironment for bone growth from purified human pericytes delivered on hCBC scaffolds. Nevertheless, the utilization of the intramuscular transplantation mouse model not only remarkably simplifies, but also improves data interpretation in defining the osteogenic property of human pericytes with and without Nell-1 enhancement *in vivo*. rhNell-1 presence markedly upregulated *Runx2, Osx,* and *Ocn* gene expression and mineralization in pericytes. Nell-1 is a highly osteospecific molecule that is directly regulated by Runx2, the master regulatory gene for osteoblast differentiation.[46]

rhNell-1 also significantly enhanced the inherent angiogenic property of pericytes. *In vitro* and *in vivo* VEGF production by human pericytes as well as angiogenesis were greatly upregulated in the presence of Nell-1. Improved angiogenesis in rhNell-1 +pericyte groups likely contributed to more effective bone regeneration as the osteogenic-angiogenic interface in bone biology is well described.[47] Consistent with this, enhanced osteogenesis, ascribed to increased VEGF secretion, was observed in human umbilical vein endothelial cells and human osteoprogenitor (HOP) cells co-cultures relative to HOP monocultures.[48] Meanwhile, the co-application of adenoviral VEGF-transduced ADSC with endothelial progenitor cells also significantly improved bone repair *in vivo.*[49] Lastly, the observed human pericyte engraftment into small blood vessels in the regenerates further supports the significant role of vascular ingrowth and angiogenesis in promoting bone regeneration in our pericyte/rhNell-1 implant models. Overall, our data offer direct experimental evidence that Nell-1 enhances VEGF expression and angiogenesis during bone regeneration.

Advantages of using homogenously purified human pericytes (CD146+, CD34−, CD45−, CD56−) over conventional hMSC include but are not limited to: (1) precise characterization in terms of native tissue localization, phenotype, and developmental potential, whereas the most frequently used hMSC are from bone marrow (BMSC) and are retrospectively derived from primary, heterogeneous cell cultures based on their plastic adherence property; (2) no *ex vivo* culture of purified pericytes is absolutely required, but these pericytes can be expanded into large amounts in a short time *in vitro* without alteration of their MSC characteristics,[14] whereas BMSC have to be cultivated and passaged at very limited numbers in plastic vessels *in vitro* over certain periods before being applicable; (3) improved trophic potency over classically derived adipose tissue and cord blood MSC[18]; and (4) the inherent function of pericytes in regulating endothelial cell proliferation, differentiation, survival, and capillary tube formation to promote angiogenesis and tissue ingrowth during regeneration. Practically, the collection of highly purified human pericytes and its long-term storage in liquid nitrogen, much like cord blood, peripheral blood, or bone marrow, could be expected for future use in personalized reparative and regenerative medicine of the skeleton as well as other mesodermal tissues.

Important limitations exist toward the broader extrapolation of these results to clinical practice. First, PSCs were derived from a single biological specimen (given the difficulty in obtaining human fetal tissue). While this study is proof-of-principle demonstration that pancreatic-derived PSCs are able to undergo osteogenesis, there is no data yet known regarding potential biological variability based on gender, age, or other demographic data. In addition, PSCs were explanted in an ectopic environment, rather than in a bone defect (orthotopic) microenvironment. Studies have suggested that the bone defect niche is critical for MSC-mediated bone formation. Thus, we consider a second set of experiments of vital importance where PSCs are explanted in a bone defect scenario to assess true clinical applicability.

Conclusion

Homogenously purified human pericytes exhibited potent osteogenic potential and direct involvement in new bone regeneration and angiogenesis; rhNell-1 significantly enhanced these effects. We demonstrated here the feasibility and efficacy of combining perivascular stem cells and rhNell-1 on an osteoconductive hCBC scaffold to promote better bone formation and vascular ingrowth. These and similar methods may be useful in future efforts in bone repair and regeneration.

Acknowledgments

This work was supported by the NIH/NIDCR (grants R21 DE0177711 and RO1 DE01607), UC Discovery Grant 07.10677, and the Thomas R. Bales Endowed Chair. M.C. was supported by the California Institute for Regenerative Medicine Training Grant (TG2-01169). A.W.J. was supported by T32 grant number 5T32DE007296-14.

Disclosure Statement

Drs. X.Z., K.T., and C.S. are inventors of Nell-1-related patents and K.T., B.P., and C.S. are inventors of a perivascular stem cell patent filed from UCLA. Drs. X.Z., K.T., and

C.S., are founders of Bone Biologics Inc., which sublicenses Nell-1 patents from UC Regents and Drs. K.T. and C.S. are founders of Scarless Laboratories, Inc., which intends to sublicence a perivascular stem cell patent filed from the UC Regents.

References

1. Rahaman, M.N., and Mao, J.J. Stem cell-based composite tissue constructs for regenerative medicine. Biotechnol Bioeng **91,** 261, 2005.
2. Perri, B., Cooper, M., Lauryssen, C., and Anand, N. Adverse swelling associated with use of rh-BMP-2 in anterior cervical discectomy and fusion: a case study. Spine J **7,** 235, 2007.
3. Shields, L.B., Raque, G.H., Glassman, S.D., Campbell, M., Vitaz, T., Harpring, J., *et al.* Adverse effects associated with high-dose recombinant human bone morphogenetic protein-2 use in anterior cervical spine fusion. Spine **31,** 542, 2006.
4. Poynton, A.R., and Lane, J.M. Safety profile for the clinical use of bone morphogenetic proteins in the spine. Spine **27,** S40, 2002.
5. Caplan, A.I. New era of cell-based orthopedic therapies. Tissue Eng Part B Rev **15,** 195, 2009.
6. Meliga, E., Strem, B.M., Duckers, H.J., and Serruys, P.W. Adipose-derived cells. Cell Transplant **16,** 963, 2007.
7. Rosland, G.V., Svendsen, A., Torsvik, A., Sobala, E., McCormack, E., Immervoll, H., *et al.* Long-term cultures of bone marrow-derived human mesenchymal stem cells frequently undergo spontaneous malignant transformation. Cancer Res **69,** 5331, 2009.
8. Cheung, W.K., Working, D.M., Galuppo, L.D., and Leach, J.K. Osteogenic comparison of expanded and uncultured adipose stromal cells. Cytotherapy **12,** 554, 2010.
9. Muller, A.M., Mehrkens, A., Schafer, D.J., Jaquiery, C., Guven, S., Lehmicke, M., *et al.* Towards an intraoperative engineering of osteogenic and vasculogenic grafts from the stromal vascular fraction of human adipose tissue. Eur Cell Mater **19,** 127, 2010.
10. Garcia-Olmo, D., Herreros, D., Pascual, M., Pascual, I., De-La-Quintana, P., Trebol, J., *et al.* Treatment of enterocutaneous fistula in Crohn's Disease with adipose-derived stem cells: a comparison of protocols with and without cell expansion. Int J Colorectal Dis **24,** 27, 2009.
11. Rajashekhar, G., Traktuev, D.O., Roell, W.C., Johnstone, B.H., Merfeld-Clauss, S., Van Natta, B., *et al.* IFATS collection: adipose stromal cell differentiation is reduced by endothelial cell contact and paracrine communication: role of canonical Wnt signaling. Stem Cells **26,** 2674, 2008.
12. Meury, T., Verrier, S., and Alini, M. Human endothelial cells inhibit BMSC differentiation into mature osteoblasts *in vitro* by interfering with osterix expression. J Cell Biochem **98,** 992, 2006.
13. Bianco, P., and Robey, P.G. Stem cells in tissue engineering. Nature **414,** 118, 2001.
14. Crisan, M., Yap, S., Casteilla, L., Chen, C.W., Corselli, M., Park, T.S., Andriolo, G., Sun, B., Zheng, B., Zhang, L., Norotte, C., Teng, P.N., Traas, J., Schugar, R., Deasy, B.M., Badylak, S., Buhring, H.J., Giacobino, J.P., Lazzari, L., Huard, J., and Péault, B. A perivascular origin for mesenchymal stem cells in multiple human organs. Cell Stem Cell **11,** 301, 2008.
15. Crisan, M., Chen, C.W., Corselli, M., Andriolo, G., Lazzari, L., and Péault, B. Perivascular multipotent progenitor cells in human organs. Ann NY Acad Sci **1176,** 118, 2009.
16. De Ugarte, D.A., Morizono, K., Elbarbary, A., Alfonso, Z., Zuk, P.A., Zhu, M., *et al.* Comparison of multi-lineage cells from human adipose tissue and bone marrow. Cells Tissues Organs **174,** 101, 2003.
17. Aust, L., Devlin, B., Foster, S.J., Halvorsen, Y.D., Hicok, K., du Laney, T., *et al.* Yield of human adipose-derived adult stem cells from liposuction aspirates. Cytotherapy **6,** 7, 2004.
18. Chen, C.W., Montelatici, E., Crisan, M., Corselli, M., Huard, J., Lazzari, L., and Péault, B. Perivascular multi-lineage progenitor cells in human organs: regenerative units, cytokine sources or both? Cytokine Growth Factor Rev **20,** 429, 2009
19. Decker, B., Bartels, H., and Decker, S. Relationships between endothelial cells, pericytes, and osteoblasts during bone formation in the sheep femur following implantation of tricalciumphosphate-ceramic. Anat Rec **242,** 310, 1995.
20. Schor, A.M., Allen, T.D., Canfield, A.E., Sloan, P., and Schor, S.L. Pericytes derived from the retinal microvasculature undergo calcification *in vitro*. J Cell Sci **97 (Pt 3),** 449, 1990.
21. Canfield, A.E., Doherty, M.J., Wood, A.C., Farrington, C., Ashton, B., Begum, N., *et al.* Role of pericytes in vascular calcification: a review. Z Kardiol **89 Suppl 2,** 20, 2000.
22. Desai, J., Shannon, M.E., Johnson, M.D., Ruff, D.W., Hughes, L.A., Kerley, M.K., *et al.* Nell1-deficient mice have reduced expression of extracellular matrix proteins causing cranial and vertebral defects. Hum Mol Genet **15,** 1329, 2006.
23. Lu, S.S., Whang, J., Zhang, X., Wu, B., Turner, A.S., Seim, H.B., *et al.* NELL-1 promotes bone formation in a sheep spinal fusion model. J Bone Miner Res **23,** S171, 2007.
24. Lu, S.S., Zhang, X., Soo, C., Hsu, T., Napoli, A., Aghaloo, T., *et al.* The osteoinductive properties of Nell-1 in a rat spinal fusion model. Spine J **7,** 50, 2007.
25. Cowan, C.M., Cheng, S., Ting, K., Soo, C., Walder, B., Wu, B., *et al.* Nell-1 induced bone formation within the distracted intermaxillary suture. Bone **38,** 48, 2006.
26. Aghaloo, T., Cowan, C.M., Chou, Y.-F., Zhang, X., Lee, H., Miao, S., *et al.* Nell-1-induced bone regeneration in calvarial defects. Am J Pathol **169,** 903, 2006.
27. Aghaloo, T., Jiang, X., Soo, C., Zhang, Z., Zhang, X., Hu, J., *et al.* A study of the role of Nell-1 gene modified goat bone marrow stromal cells in promoting new bone formation. Mol Ther **15,** 1872, 2007.
28. Cowan, C.M., Jiang, X., Hsu, T., Soo, C., Zhang, B., Wang, J.Z., *et al.* Synergistic effects of Nell-1 and BMP-2 on the osteogenic differentiation of myoblasts. J Bone Miner Res **22,** 918, 2007.
29. Parfitt, A.M., Drezner, M.K., Glorieux, F.H., Kanis, J.A., Malluche, H., Meunier, P.J., *et al.* Bone histomorphometry: standardization of nomenclature, symbols, and units. Report of the ASBMR Histomorphometry Nomenclature Committee. J Bone Miner Res **2,** 595, 1987.
30. Muller, R., and Ruegsegger, P. Micro-tomographic imaging for the nondestructive evaluation of trabecular bone architecture. Stud Health Technol Inform **40,** 61, 1997.
31. Gauthier, O., Muller, R., von Stechow, D., Lamy, B., Weiss, P., Bouler, J.M., *et al. In vivo* bone regeneration with injectable calcium phosphate biomaterial: a three-dimensional micro-computed tomographic, biomechanical and SEM study. Biomaterials **26,** 5444, 2005.
32. James, A.W., Theologis, A.A., Brugmann, S.A., Xu, Y., Carre, A.L., Leucht, P., *et al.* Estrogen/estrogen receptor alpha signaling in mouse posterofrontal cranial suture fusion. PLoS One **4,** e7120, 2009.

33. Shoji, T., Li, M., Mifune, Y., Matsumoto, T., Kawamoto, A., Kwon, S.M., Kuroda, T., Kuroda, R., Kurosaka, M., and Asahara, T. Local transplantation of human multipotent adipose-derived stem cells accelerates fracture healing via enhanced osteogenesis and angiogenesis. Lab Invest **90,** 637, 2010.
34. Covas, D.T., Panepucci, R.A., Fontes, A.M., Silva, W.A., Jr., Orellana, M.D., Freitas, M.C., *et al.* Multipotent mesenchymal stromal cells obtained from diverse human tissues share functional properties and gene-expression profile with CD146+ perivascular cells and fibroblasts. Exp Hematol **36,** 642, 2008.
35. Huang, G.T., Gronthos, S., and Shi, S. Mesenchymal stem cells derived from dental tissues vs. those from other sources: their biology and role in regenerative medicine. J Dent Res **88,** 792, 2009.
36. da Silva Meirelles, L., Sand, T.T., Harman, R.J., Lennon, D.P., and Caplan, A.I. MSC frequency correlates with blood vessel density in equine adipose tissue. Tissue Eng Part A **15,** 221, 2009.
37. da Silva Meirelles, L., Caplan, A.I., and Nardi, N.B. In search of the *in vivo* identity of mesenchymal stem cells. Stem Cells **26,** 2287, 2008.
38. Shi, S., and Gronthos, S. Perivascular niche of postnatal mesenchymal stem cells in human bone marrow and dental pulp. J Bone Miner Res **18,** 696, 2003.
39. Corselli, M., Chen, C.W., Crisan, M., Lazzari, L., and Péault, B. Perivascular ancestors of adult multipotent stem cells. Arterioscler Thromb Vasc Biol **30,** 1104, 2010.
40. Tedesco, F.S., Dellavalle, A., Diaz-Manera, J., Messina, G., and Cossu, G. Repairing skeletal muscle: regenerative potential of skeletal muscle stem cells. J Clin Invest **120,** 11, 2010.
41. Cai, X., Lin, Y., Friedrich, C.C., Neville, C., Pomerantseva, I., Sundback, C.A., Zhang, Z., Vacanti, J.P., Hauschka, P.V., and Grottkau, B.E. Bone marrow derived pluripotent cells are pericytes which contribute to vascularization. Stem Cell Rev **5,** 437, 2009.
42. Zheng, B., Cao, B., Crisan, M., Sun, B., Li, G., Logar, A., *et al.* Prospective identification of myogenic endothelial cells in human skeletal muscle. Nat Biotechnol **25,** 1025, 2007.
43. Zhang, X., Carpenter, D., Bokui, N., Soo, C., Miao, S., Truong, T., *et al.* Overexpression of Nell-1, a craniosynostosis-associated gene, induces apoptosis in osteoblasts during craniofacial development. J Bone Miner Res **18,** 2126, 2003.
44. Zhang, X., Kuroda, S., Carpenter, D., Nishimura, I., Soo, C., Moats, R., *et al.* Craniosynostosis in transgenic mice overexpressing Nell-1. J Clin Invest **110,** 861, 2002.
45. Lin, L., Shen, Q., Wei, X., Hou, Y., Xue, T., Fu, X., *et al.* Comparison of osteogenic potentials of BMP4 transduced stem cells from autologous bone marrow and fat tissue in a rabbit model of calvarial defects. Calcif Tissue Int **85,** 55, 2009.
46. Truong, T., Zhang, X., Pathmanathan, D., Soo, C., Ting, K. Craniosynostosis-associated gene Nell-1 is regulated by Runx2. J Bone Miner Res **22,** 7, 2007.
47. Towler, D.A. The osteogenic-angiogenic interface: novel insights into the biology of bone formation and fracture repair. Curr Osteoporos Rep **6,** 67, 2008.
48. Grellier, M., Granja, P.L., Fricain, J.C., Bidarra, S.J., Renard, M., Bareille, R., *et al.* The effect of the co-immobilization of human osteoprogenitors and endothelial cells within alginate microspheres on mineralization in a bone defect. Biomaterials **30,** 3271, 2009.
49. Jabbarzadeh, E., Starnes, T., Khan, Y.M., Jiang, T., Wirtel, A.J., Deng, M., *et al.* Induction of angiogenesis in tissue-engineered scaffolds designed for bone repair: a combined gene therapy-cell transplantation approach. Proc Natl Acad Sci USA **105,** 11099, 2008.

Address correspondence to:
Chia Soo, M.D.
Department of Orthopaedic Surgery
University of California, Los Angeles
675 Charles E Young Dr South
MRL 2641A
Los Angeles, CA 90095-1579

E-mail: bsoo@ucla.edu

Received: December 3, 2010
Accepted: May 25, 2011
Online Publication Date: July 14, 2011